Manipulation of the surface density of states of Ag(111) by means of resonators: Experiment and theory

J. Fernández,[1] María Moro-Lagares,[2,3,4] D. Serrate,[5,6] and A. A. Aligia[1]

[1]*Centro Atómico Bariloche and Instituto Balseiro, Comisión Nacional de Energía Atómica, 8400 Bariloche, Argentina*

[2]*Laboratorio de Microscopias Avanzadas, Instituto de Nanociencia de Aragón, University of Zaraqoza, E-50018 Zaragoza, Spain*

[3]*Institute of Physics, Academy of Sciences, Prague, Czech Republic*

[4]*Regional Centre of Advanced Technologies and Materials, Faculty of Science, Department of Physical Chemistry, Palacky University, Olomouc, Czech Republic*

[5]*Instituto de Nanociencia de Aragón, Laboratorio de Microscopias Avanzadas, University of Zaraqoza, E-50018 Zaragoza, Spain*

[6]*Departamento Física Materia Condensada, University of Zaraqoza, E-50018 Zaragoza, Spain*

(Received 24 May 2016; published 8 August 2016)

We show that the density of surface Shockley states of Ag(111) probed by the differential conductance $G(V) = dI/dV$ by a scanning-tunneling microscope (STM) can be enhanced significantly at certain energies and positions introducing simple arrays of Co or Ag atoms on the surface, in contrast to other noble-metal surfaces. Specifically we have studied resonators consisting of two parallel walls of five atoms deposited on the clean Ag(111) surface. A simple model in which the effect of the adatoms is taken into account by an attractive local potential and a small hybridization between surface and bulk at the position of the adatoms explains the main features of the observed $G(V)$ and allows us to extract the proportion of surface and bulk states sensed by the STM tip. These results might be relevant to engineer the surface spectral density of states, to study the effects of surface states on the Kondo effect, and to separate bulk and surface contributions in STM studies of topological surface states.

DOI: 10.1103/PhysRevB.94.075408

I. INTRODUCTION

Research using a scanning-tunneling microscope (STM) has enabled the manipulation of single atoms or molecules on top of a surface [1] and the construction of structures of arbitrary shape such as quantum corrals [2–4]. Moreover, the differential conductance $G(V,\mathbf{r}) = dI/dV$ measured by the STM at position $\mathbf{r}$, where I is the current and V the applied voltage is in general proportional to the local density of metal states [5,6]. However, the bulk and surface contributions to this electronic density are weighted differently by the STM tip due to the different decay rate of the wave functions out of the surface [7]. More recently, the STM has been used to study the surface states of topological insulators [8]. For the interpretation of these experiments it would be very important to separate bulk and surface contributions. Interestingly, the effect of the different distance dependence of tunneling processes involving $3d$ and s/p states has been observed recently for Fe_2N on Cu(001) [9].

The (111) surfaces of Cu, Ag, and Au have the property that for small wave vectors parallel to the surface a parabolic band of two-dimensional surface states, confined to the last few atomic planes and uncoupled to bulk states, exists [10]. The surface states are naturally more sensitive to defects or impurities at the surface and this fact can be used to modify the surface density of electronic states. In a famous experiment, a Co atom acting as a magnetic impurity was placed at one focus of an elliptical quantum corral built on the Cu(111) surface. A Fano-Kondo antiresonance (which arises when a magnetic impurity interacts with a continuum of extended states) was observed in $G(V)$ not only at that position, but also with reduced intensity at the other focus [4]. This "mirage" can be understood as the result of quantum interference in the way in which the Kondo effect is transmitted from one focus to the other by the different eigenstates of surface conduction electrons inside a hard-wall ellipse [6,11–16]. This experiment already shows that the confinement of surface states has dramatic consequences on the Kondo effect, although some experiments suggest that the screening of the impurity spin by the bulk conduction electrons plays the dominant role in this effect [17]. From the mirage intensity it has been estimated that the coupling to the surface states is at least 1/8 that of the bulk [6]. Predictions of the variation of the Kondo temperature T_K with the position of the impurity were made [6,18].

On the other hand, while the eigenstates inside a hard wall corral are perfectly defined, in the actual experiments the boundaries of the corrals are soft and the eigenstates become resonances with finite width δ_i [2,19]. This width plays a crucial role in the line shape of $G(V,\mathbf{r})$ and its magnitude at the mirage point. If δ_i is large the mirage disappears, while if $\delta_i = 0$, there is no Kondo resonance at the Fermi level ϵ_F [11,15]. For a circular corral of radius r_0 with the boundary defined by a potential proportional to a delta function $\delta(r - r_0)$, where r is the distance to the center of the circle, the Green function for surface conduction electrons inside the corral G_s^0 has been obtained analytically and expanded as a discrete sum of contributions from simple poles of width δ_i [19]. For open structures this approach is not possible. An alternative approach in which the confining atoms are modeled by a phenomenological scattering approach [5] was successful for closed corrals [3].

In this paper we have constructed atomic resonators of Co and Ag by atomic lateral manipulation technique with only two walls aligned along the $[1\bar{1}0]$ direction. These atomic arrangements confine surface electrons states in such a way that the movement of the electrons near the surface is only constrained along the $[11\bar{2}]$ directions. The characteristic they all share is the distance between the Co atoms forming the wall,

which corresponds to three Ag(111) interatomic distances $d = 3a_{\mathrm{Ag}}$ ($a_{\mathrm{Ag}} = 0.29$ Å).

We show that the main features of $G(V,\mathbf{r})$ can be explained by a very simple model, the main ingredient of which is an attractive delta function potential W acting on the surface states at the position of single Co (Ag) atoms adsorbed on the Ag(111) surface. The origin of this potential is the sum of the nuclear potential of the adatom [20] and a contribution due to the hybridization of surface states with the adatom [21]. At each position, we also include an effective surface-bulk hybridization.

In Sec. II, we describe the model and the equations that determine the observed conductance. Experimental results with the corresponding theoretical ones and other theoretical results are presented in Sec. III, and Sec. IV contains a summary and discussion.

II. MODEL AND FORMALISM

A. Hamiltonian

The Hamiltonian can be written as

$$H = \sum_{\mathbf{k}\sigma} \epsilon_{\mathbf{k}} s^\dagger_{\mathbf{k}\sigma} s_{\mathbf{k}\sigma} + \sum_{\mathbf{q}\sigma} \epsilon_{\mathbf{q}} b^\dagger_{\mathbf{q}\sigma} b_{\mathbf{q}\sigma} + W \sum_{i\sigma} s^\dagger_{i\sigma} s_{i\sigma} + \sum_{i\sigma} (W_b s^\dagger_{i\sigma} b_{i\sigma} + \mathrm{H.c.}). \quad (1)$$

The first term describes a two-dimensional band of free electrons of mass 0.31 times the electron mass, which describes the Shockley surface states. It starts at 67 meV below the Fermi level which we set as the origin of energies ($\epsilon_F = 0$). [21] The second term corresponds to the three-dimensional bulk states. The third term is a potential scattering for the surface electrons at the position of each adatom (labeled by i) [22]. This term is the sum of the nuclear potential of the adatom, incompletely screened by the adatom and conduction electrons [as argued by Olsson *et al.* for Cu adatoms on Cu(111) [20]] plus a contribution $V^2_{as}/(\omega - \epsilon_a)$, where V_{as} is the hybridization between an adatom level at energy ϵ_a and the surface conduction electrons [21] (the dependence on energy ω can be neglected for ω close to the Fermi energy). The last term is an effective surface-bulk hybridization, which in terms of the model used in Ref. [21] is $W_b = V_{as}\bar{V}_{ab}/(\omega - \epsilon_a)$, where V_{ab} is the hybridization between the adatom level and the bulk conduction electrons. Thus for one adatom and $\omega \sim \epsilon_F$, our model is essentially equivalent to that used by Limot *et al.* to study the bound states below the surface band originated by one adatom [21].

The Wannier function of the band states can be written in the form

$$s_{j\sigma} = \frac{\lambda}{\sqrt{A}} \sum_{\mathbf{k}} \exp(-i\mathbf{k}\cdot\mathbf{r}_j) s_{\mathbf{k}\sigma},$$
$$b_{j\sigma} = \sqrt{\frac{\lambda^2 d}{\Omega}} \sum_{\mathbf{q}} \exp(-i\mathbf{q}\cdot\mathbf{r}_j) b_{\mathbf{q}\sigma}, \quad (2)$$

where A (Ω) is the area of the (111) surface (volume of the system), λ^2 ($\lambda^2 d$) the area (volume) per Ag atom, and $\mathbf{r}_j$ is an arbitrary position on the surface.

B. Differential conductance

At sufficiently low temperature, the differential conductance $G(V,\mathbf{r}_t)$ when the STM tip is at position $\mathbf{r}_t$ on the surface is proportional to the density of the mixed state [23,24],

$$h_\sigma(\mathbf{r}_t) = \alpha s_{t\sigma} + \beta b_{t\sigma}, \quad (3)$$

$$\frac{G(V,\mathbf{r}_t)}{C} = \rho_h(\epsilon_F + eV) = -\frac{1}{\pi}\mathrm{Im}G^\sigma_{hh}(\epsilon_F + eV), \quad (4)$$

where C is a constant, $G^\sigma_{hh}(\omega) = \langle\langle h_\sigma; h^\dagger_\sigma\rangle\rangle_\omega$ is the Green function of $h_\sigma(\mathbf{r}_t)$, and α and β with $|\alpha|^2 + |\beta|^2 = 1$ are proportional to the tunneling matrix elements between the tip and surface and bulk states, respectively. These in turn depend on the decay of the corresponding wave functions out of the surface [7]. In particular bulk states with different components of wave vector $\mathbf{q}$ perpendicular to the surface have different extents out of the surface. Thus, Eq. (3) is an oversimplification because it assumes that the tunneling matrix elements are the same for all wave vectors entering Eqs. (2). However, as we will show, it is enough for our purpose.

From Eqs. (3) and (4) one obtains (dropping the spin superscripts for simplicity

$$G_{hh} = |\alpha|^2 G_{tt} + |\beta|^2 G_{t't'} + \alpha\bar{\beta}G_{tt'} + \bar{\alpha}\beta G_{t't},$$

where primed (unprimed) subscripts refer to bulk (surface) states. For example $G_{tt'}(\omega) = \langle\langle s_{t\sigma}; b^\dagger_{t\sigma}\rangle\rangle_\omega$. For the last two interference terms, the wave vector dependence which is different for bulk and surface states plays a role. Here we assume that the phases are such that adding the contributions from different wave vectors leads to a near cancellation of these terms. The comparison with experiment suggests that this is a good approximation. Thus we assume

$$G_{hh} \simeq |\alpha|^2 G_{tt} + |\beta|^2 G_{t't'}. \quad (5)$$

C. Green functions

To obtain the surface (G_{tt}) and bulk ($G_{t't'}$) Green functions that determine the conductance through Eqs. (4) and (5) we use the Dyson equation, which in matrix form is

$$\mathbf{G} = \mathbf{G}^0 + \mathbf{G}^0\mathbf{H}'\mathbf{G}, \quad (6)$$

where $\mathbf{G}^0$ is the Green function matrix for free electrons [first two terms of Eq. (1)], and $\mathbf{H}'$ correspond to the Hamiltonian terms introduced by the adatoms [last two terms of Eq. (1)].

For the free bulk states we assume a flat broad band with a constant density of states per spin $\rho_b = 0.135/\mathrm{eV}$, which is the known value at the Fermi level. Since the free bulk Green function $G_{i'j'}$ is known to decay very rapidly with distance [17,25], we only need to use it when both operators b_i, $b^\dagger_j$ act on the same site:

$$G^0_{j'j'} = -i\pi\rho_b. \quad (7)$$

The Green function for free electrons in two dimensions is known [25]. It is proportional to a Hankel function H_0 for $\omega > \omega_B$, where $\omega_B = -67$ meV is the bottom of the conduction band, and to a (real) Bessel function of the second kind Y_0 for $\omega < \omega_B$. Therefore the other nonzero matrix elements

of $\mathbf{G}^0$ that we need are

$$\begin{aligned} G^0_{ij} &= -i\pi\rho_{s0}H_0(k|\mathbf{r}_i - \mathbf{r}_f|), \text{ if } \omega > \omega_B, \\ G^0_{ij} &= \pi\rho_{s0}Y_0(k|\mathbf{r}_i - \mathbf{r}_f|), \text{ if } \omega < \omega_B, \\ k &= [2m^*|\omega - \omega_B|]^{1/2}/\hbar, \\ \rho_{s0} &= \frac{m^*\lambda^2}{2\pi\hbar^2} \simeq 0.0466/\text{eV}, \end{aligned} \tag{8}$$

where we have used $\lambda = 0.2685$ nm.

Taking matrix elements in Eq. (6) one obtains

$$G_{lt} = G^0_{lt} + \sum_i G^0_{li}(WG_{it} + W_bG_{i't}), \tag{9}$$

$$G_{i't} = G^0_{i'i'}\bar{W}_bG_{it}, \tag{10}$$

where the sum over i runs over all adatoms, and l can refer to the tip (t) or an adatom (i) position. Replacing Eq. (10) in Eq. (9) and using Eq. (7) gives

$$G_{lt} = G^0_{lt} + \sum_i G^0_{li}(W - i\Delta)G_{it}, \tag{11}$$

$$\text{where } \Delta = \pi\rho_b|W_b|^2. \tag{12}$$

Running l over all the N adatom positions, Eqs. (11) constitute a system of N equations for the N unknowns G_{lt} that we solve numerically. Replacing this solution in Eq. (11) with $l = t$, we obtain G_{tt}. On the other hand, out of the adatom positions one has $G_{t't'} = G^0_{t't'}$. Then, using Eqs. (4) and (5) we obtain the conductance $G(V,\mathbf{r}_t)$. We use W and Δ as fitting parameters which depend only on the adatom species (Co or Ag). The other fitting parameters are the coefficients of the bulk $B = C|\beta|^2$ and surface $S = C|\alpha|^2$ contributions, which depend on the distance between the tip and the surface.

III. RESULTS

In this section we first compare experiment with theory for three resonators and then discuss other results provided by the theory. Quantum corrals are atomic structures in which the atoms are positioned forming closed geometries. Such structures are ideal to control the spatial and spectral distribution of surface electron states [6,18,26,27]. In general, the confinement of surface electrons gives rise to periodic interference patterns with alternating maxima and minima of the local density of states (LDOS) sensed by the STM tip (see Sec. II), which as we will see corresponds mainly to surface electrons. However, we are interested in building an artificial Ag(111) LDOS with the maximum possible amplitude of the LDOS oscillations. In the artificial LDOS design process both the length of the resonator's walls and the distance between each other are important parameters to take into account. In order to obtain one maximum of LDOS at the Fermi level, the one-dimensional particle-in-a-box problem sets the minimum distance between the atomic arrays d_w to a value of $\lambda_F/2$, which is 3.7 nm in the case of the Ag(111) surface. This applies for the model case, in which an infinite potential well limits the movement of a particle [28]. This will be discussed in more detail in Sec. III C. Therefore, the probability of finding the particle outside the box is zero and the wave function must be zeroed at the walls. In this work, the resonator's walls do not form an infinite barrier; they have a certain permeability and the optimum distance between the walls is expected to be different. Furthermore, in order to prevent any electron correlation effect between the atomic arrays, we look for the maximum distance between the walls at which the target LDOS maximum is preserved. For this purpose, we construct three different atomic resonators (Fig. 1).

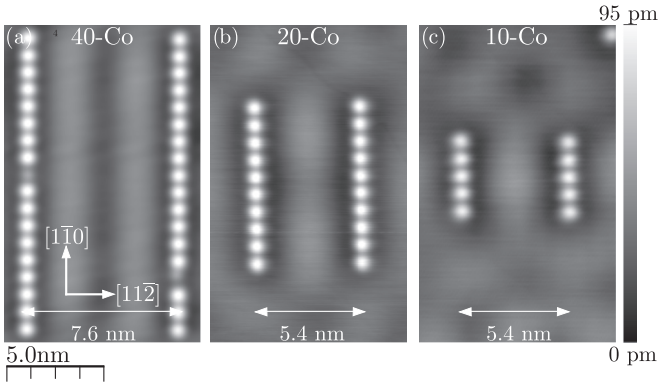

FIG. 1. Topographic images of three Co resonators with atoms at $d_{Co\text{-}Co} = 3a$. (a) 40-Co resonator with atomic walls at $d_w = 7.6$ nm showing two maxima of the LDOS along the [11$\bar{2}$] direction ($I_T = 200$ pA, $V_{\text{bias}} = 50$ mV). (b) 20-Co resonator with walls at $d_w = 5.4$ nm showing two maxima along the [1$\bar{1}$0] closed packed direction ($I_T = 200$ pA, $V_{\text{bias}} = 10$ mV). (c) 10-Co resonator with atomic walls built at $d_w = 5.4$ nm. This atomic arrangement gives rise to a unique maximum along the [1$\bar{1}$0] closed packed direction ($I_T = 500$ pA, $V_{\text{bias}} = 10$ mV).

In Fig. 1 we show the topographic image of three different atomic resonators of different lengths [see Figs. 1(a)–1(c)] and walls spacing [Figs. 1(a) and 1(b)]. We choose d_w by comparing the conductance maps at the Fermi energy of the 40 and 10-Co resonators [Figs. 2(a) and 2(b)]. The former shows a unique central maximum while the latter exhibits a complex alternating pattern of maxima and minima along the [1$\bar{1}$0] and [11$\bar{2}$] directions. Moreover, comparing the line profiles [Fig. 2(c)] taken in both resonators, it is found that the artificial Ag(111) LDOS is more intense in the resonator with walls at $d_w = 5.4$ nm. On the other hand, the wall length is set after observing that the two central maxima of the 20 atoms resonator consists in simply repeating the structure of the 10-atom resonator [Figs. 1(b) vs 1(c)]. Therefore, we select the resonator with five atoms forming the walls and $d_w = 5.4$ nm as the optimal geometry to tailor the artificial Ag(111) LDOS.

In order to characterize the artificially engineered LDOS inside the resonator, by means of scanning tunneling spectroscopy (STS), we experimentally measure and theoretically calculate the relevant spectral signatures of the modified Ag(111) surface. For each position of the tip we define V_{Max} as the voltage for which the conductance $G(V)$ is maximum and V_{Onset} as the relative maximum of $dG/dV = d^2I/dV^2$ for $V < V_{\text{Max}}$. In Fig. 3 we show the evolution of $G(0)$, V_{Onset}, and V_{Max} as the STM tip moves along the symmetry axis parallel to the walls of the resonator. For the amplitude of the surface contribution S in the theoretical calculation, we have taken the value obtained from the fits described in the next subsections near the center of the resonator. This implies

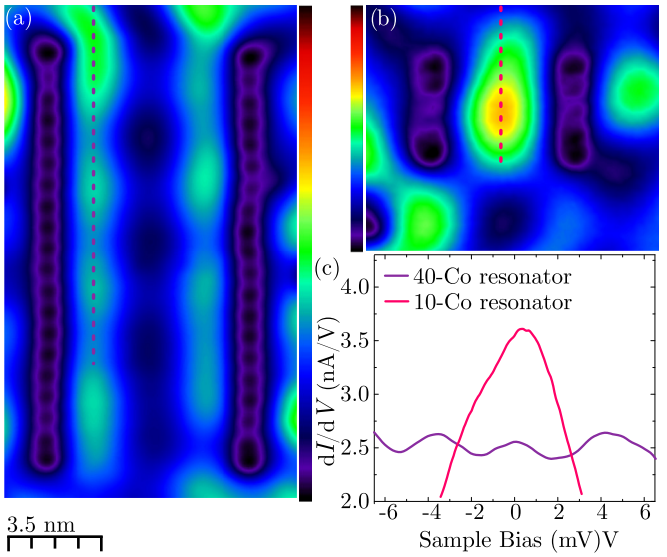

FIG. 2. dI/dV map at the Fermi level ($V = 0$) of Co resonators with atomic walls with different numbers of atoms and wall distances, d_w. (a) 40-Co resonator with $d_w = 7.4$ nm (regulation set point: $I_T = 200$ pA, $V = -100$ mV $V_{\text{mod}} = 3$ mV) showing an alternating maximum/minimum pattern of the Ag(111) LDOS along the $[1\bar{1}0]$ and the $[11\bar{2}]$ directions. (b) Conductance map at the Fermi energy of a 10-Co resonator with $d_w = 5.4$ nm (regulation set point: $I_T = 200$ pA, $V = -100$ mV; $V_{\text{mod}} = 3$ mV) showing only one maximum of the Ag(111) LDOS. (c) Line profiles along the $[1\bar{1}0]$ directions [dotted lines in (a) and (b)] showing a more intense maximum in the resonator with walls separated $d_w = 5.4$ nm.

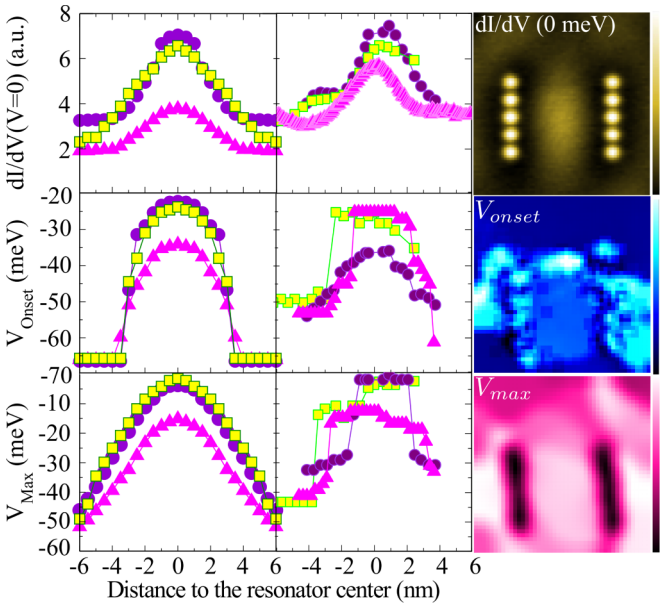

FIG. 3. Theoretically calculated (left) and experimentally measured (middle) $G(0)$, V_{Onset}, and V_{Max} (see text) as the STM tip moves along the resonator for the first Co resonator (triangles), the second Co resonator (squares), and the Ag resonator (circles). The experimental data correspond to the line profiles measured in images (examples in the right panel) generated from a full differential conductance map taken at $V_{\text{bias}} = -20$ mV, $I_T = 500$ pA, and $V_{\text{mod}} = 1$ mV or a constant height image defined by a regulation set point $I_T = 42$ pA, $V_{\text{bias}} = -100$ mV on the bare Ag(111). The symbol and color code indicates data extracted from the same resonator.

that in a more realistic calculation, higher results for $G(0)$ are expected for the experiment as the tip moves away from the center, since S increases by ~30% for the Co resonators and by a factor ~2 for the Ag one outside the resonator. In any case, except for slight discrepancies caused by inhomogeneities of the substrate, the experimentally and theoretically predicted variations of these parameters are in good agreement. For two resonators V_{Onset} is rather constant inside the resonator and rapidly falls towards the onset of surface states for a clean Ag surface ($\omega_B = -67$ meV) as the tip moves outside the resonator. In the next two subsections, we describe in more detail the observed voltage dependence of the differential conductance $G(V)$, ad its theoretical counterpart, for two Co resonators and one Ag resonator.

A. Co resonators

In Fig. 4 we present the experimental differential conductance for a Co resonator and compare it with the theoretical one for two positions of the STM tip, one inside the resonator and the other outside it. As shown in the figure, the resonator is composed of two walls of five atoms with a total length of 3.46 nm at a distance of 5.45 nm between them. The tip positions $\mathbf{r}_t$ for which the conductance $G(V,\mathbf{r}_t)$ as a function of energy $\omega = eV$ is shown to correspond to distances $d = 0.23$ nm and $d = 4.77$ nm from the center of the resonator, respectively, along the symmetry axis parallel to the walls (see the inset of Fig. 4). The fitting parameters for both positions are $W = -0.402$ eV, $\Delta = 0.0194$ eV, and the bulk prefactor $B = C|\beta|^2 = 3.72$ in the arbitrary units of the experiment. For the ratio of surface and bulk prefactors we find $S/B = |\alpha|^2/|\beta|^2 = 12.23$ inside the resonator and 13.92 outside it. This difference is probably due to the fact that the tip should be displaced towards the surface when the tip is outside the resonator, to keep the same total current, and as a consequence

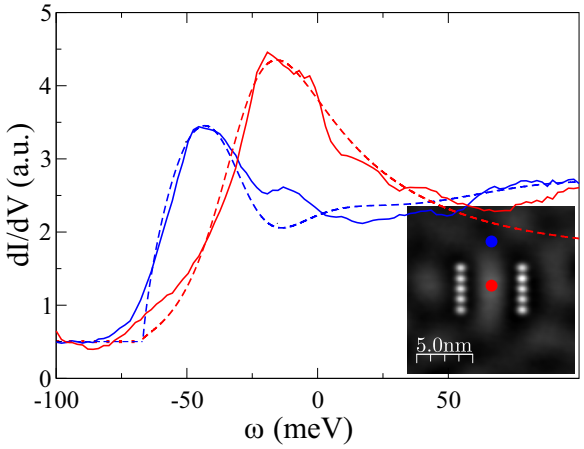

FIG. 4. Differential conductance as a function of voltage times electric charge ($\omega = eV$) for the first Co resonator and two positions of the STM tip: near the center (red, peak nearest to $\omega = 0$) and slightly outside the resonator (blue). Full (dashed) line correspond to experiment (theory, see text).

the tunneling of the surface states increases, while for the bulk states with flatter decay out of the surface, the tunneling rate does not change very much [7].

As seen in the figure, the peaks for both positions are very well reproduced by the theory, for which below the bottom of the surface band $\omega_B = -67$ meV, only the bulk contributes to the conductance. The surface contribution starts from zero at $\omega = \omega_B$ and increases abruptly. Experimentally this increase is smoother with more spectral weight at lower energies. This might be due to additional broadening processes not accounted for in our theory.

As discussed in Sec. III C, the conductance at high energies or large distances from the resonator is $B\rho_b + S\rho_{s0}$, which in this case, using the value of S for the tip near the center of the resonator is 2.62 arbitrary units. As seen in Fig. 4, this value increases 70% as a consequence of the confinement. This is due to a 100% increase in the surface density of states.

The sensitivity of the theoretical results to the bulk and surface amplitudes B and S is obvious. Increasing Δ leads to an additional broadening of the peaks. The changes in the conductance when the remaining free parameter W is changed is shown in Fig. 5. A positive W leads always to a strong disagreement with experiment. Increasing the magnitude of the attractive potential displaces the peak in the conductance to lower energies. A change of W by 15% leads to an obvious change in the position of the peak for both positions of the STM tip.

In Fig. 6, we compare experiment and theory for another Co resonator, in which the distance between the five-atom walls was reduced to 5.316 nm. In this case, the distance of

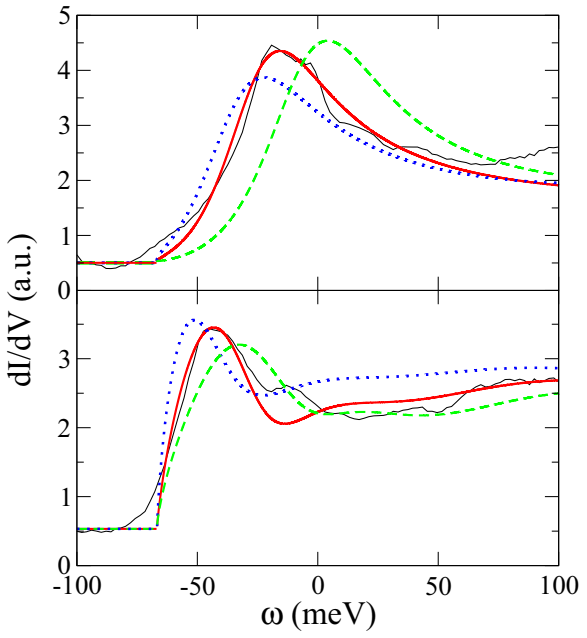

FIG. 5. Theoretical differential conductance as a function of energy for the first Co resonator, the STM tip near the center (top) red, and slightly outside the resonator (bottom), and three different values of the potential W: -0.342 eV (dashed green line), -0.402 eV (full red line), and -0.462 eV (dot blue line). Full black line corresponds to experiment.

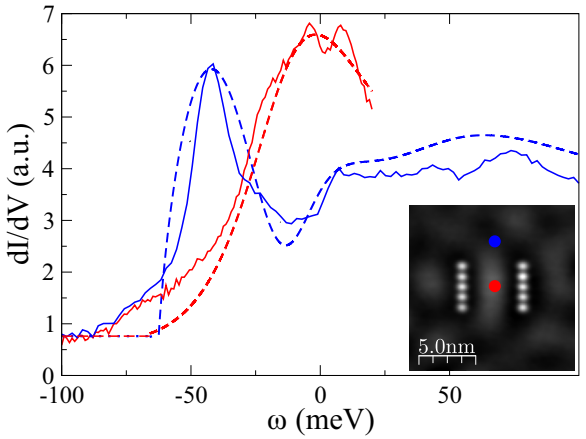

FIG. 6. Differential conductance as a function of energy for the second Co resonator and two positions of the STM tip: near the center (red, peak nearest to $\omega = 0$) and outside the resonator (blue). Full (dashed) line corresponds to experiment (theory).

the position of the tip to the center of the resonator was $d = 0$ (inside the resonator) and $d = 5.73$ nm (outside). We take the same energy parameters as before. Concerning the intensities, the fit gives $B = 5.64$ for both positions, and $S/B = 12.52$ inside the resonator and 16.69 outside it. Again, the position of the peaks are well reproduced by the theory. However, the peak for the tip inside (outside) the resonator seems to be broader (narrower) in the experiment, and the experimental surface contribution below ω_B (absent in the theory) is larger for this resonator than for the previous one. We must warn that the density of states of the tip is not expected to be constant in a broad energy range, and this might be the reason for some discrepancies.

B. Ag resonator

In Fig. 7 we present experimental results and the corresponding fit for an Ag resonator with walls at a distance $d_w = 5.33$ nm between them, as shown in the figure. The

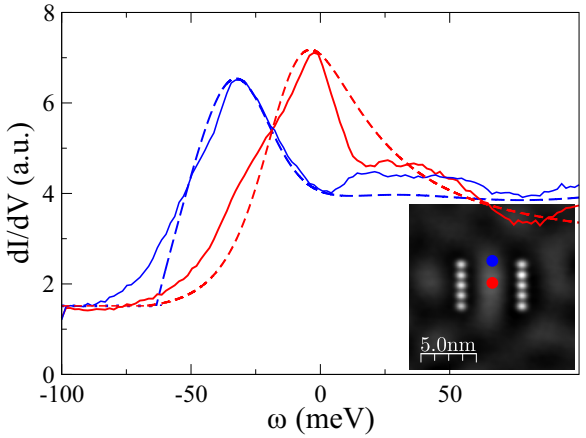

FIG. 7. Differential conductance as a function of energy for the Ag resonator and two positions of the STM tip: near the center (red, peak nearest to $\omega = 0$) and slightly outside the resonator (blue). Full (dashed) line corresponds to experiment (theory).

distance of the tip to the center of the resonator for the two positions chosen is $d = 0.36$ nm (inside the resonator) and $d = 2.47$ nm (outside). For both positions, the resulting fitting parameters are $W = -0.430$ eV, $\Delta = 0.0139$ eV, and $B = 10.56$. The ratio $S/B = 5$ for the tip inside the resonator and $S/B = 8.73$ outside it. The resulting scattering potential W that leads to the correct position of the peaks for both positions is about 7% larger than for the Co atoms. Instead the broadening due to surface-bulk hybridization Δ is 28% smaller.

While the position of the peaks and the overall trends are well reproduced by the theory, the experiment shows more spectral weight at smaller energies. The surface spectral weight for $\omega < \omega_B$, which is particularly apparent for the tip outside the resonator, cannot be explained by our theory.

The surface density of states inside the resonator increases by a factor 2.4 with respect to the value for a clean surface. For the Co resonators the corresponding factor is near 1.8.

C. Other theoretical results

Having established the parameters of the model by fitting experimental results, in this section we address some questions. Where are the bound states below the surface band? How does the conductance $G(V,\mathbf{r}_t)$ change moving the tip away from the resonator? How does $G(V,\mathbf{r}_t)$ look in an extended voltage range? Is it possible to increase further the surface density of states?

One of the consequences of an attractive potential for a steplike spectral density such as that of the surface states is the appearance of bound states below the bottom of the surface band ω_B [20,21]. In Fig. 8 we show the density of surface states when the tip is above one adatom for the first Co resonator and the Ag one (it is practically independent on the particular adatom chosen). Although the contribution of the bulk states to the conductance is very small, we should note that the surface contribution is not proportional to the expected experimental conductance because the latter includes the contribution of the adatom itself [21], which can be safely neglected for other positions, but not when the tip is on the adatom (see for example the inset of Fig. 8). Our purpose is to show the effect of the attractive potential on the surface states, originating bound states, which can be noticed only when the tip is quite close to an adatom (note the absence of peaks below ω_B in all other figures). The bound states have a finite width due to the effect of the surface-bulk hybridization W_b, which is smaller for the Ag resonator. The peak in $G(V,\mathbf{r}_t)$ is at 12.25 meV below ω_B for the Ag resonator and the corresponding value for the Co resonator is 8.57 meV. For $W_b = 0$, the corresponding values are 11.94 meV and 8.34 meV, respectively. As expected, the binding energy is larger for Ag adatoms, because of the ∼7% larger magnitude of the attractive potential W.

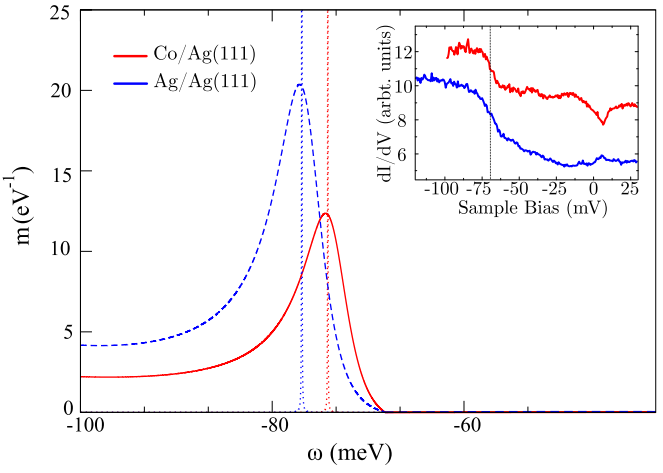

FIG. 8. Spectral density of surface states as a function of energy for the STM tip above one of the adatoms that form the Ag (full red line) and the first Co (dashed blue line) resonator. Dotted lines denote the result for a smaller $W_b = 0.001$ meV. The inset shows the energy resolved dI/dV spectra of single Ag and Co adatoms on Ag(111) taken at $V_{\text{bias}} = -100$ mV, $I_t = 200$ pA and $V_{\text{bias}} = -100$ mV, $I_t = 70$ pA, respectively. Both dI/dV curves present the split-off bound state around 75 mV below the Fermi energy. In addition, the Co atom on Ag(111) spectra presents a second resonance near the Fermi level due to the Kondo effect.

In Fig. 9 we show the conductance that corresponds to the Ag resonator described above, for three distances of the tip to the center of the resonator, moving the tip along the symmetry axis between the walls of the resonator. For a very large distance ($|\mathbf{r}_t| \to \infty$), $G(V,\mathbf{r}_t)$ has the known form for a clean surface [20,21]. Below the bottom of the surface band at $eV = \omega_B = -67$ meV, only the bulk contributes to the conductance by an amount proportional to $B\rho_b = 1.43$. Exactly at ω_B, the constant surface contribution of magnitude proportional to $S\rho_{s0} = 4.29$ begins. As the tip is moved towards the resonator, some oscillations appear in the surface contribution which becomes more intense and more separated in energy as the resonator is approached. For the tip at a distance of 2.47 nm from the center of the resonator, only one peak is present for $\omega < 100$ meV (see Fig. 7).

In Fig. 10 we show the theoretical results that correspond to the experiment for the tip inside the Ag resonator (shown before in Fig. 7) in an extended energy range. In addition to the previous peak at ~ -8 meV, another one at 350 meV is clearly seen. One might expect that these peaks are

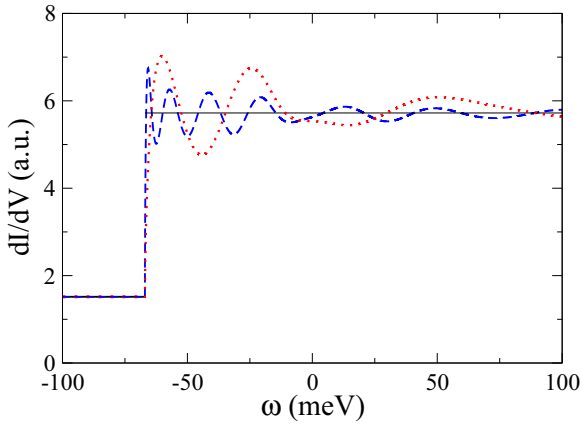

FIG. 9. Theoretical differential conductance as a function of energy for the Ag resonator and three distances d of the STM tip to the center of the resonator: $d = 10$ nm (dot red line), $d = 20$ nm (dashed blue line), and $d \to \infty$ (full black line).

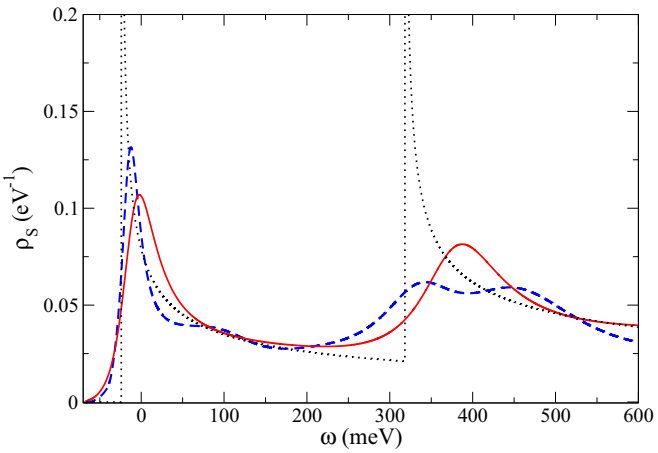

FIG. 10. Full line: theoretical differential conductance as a function of energy for the STM tip in the center of the Ag resonator. Dashed line: the same for an Ag resonator with two times longer walls. Dotted line: the same for two infinite hard walls.

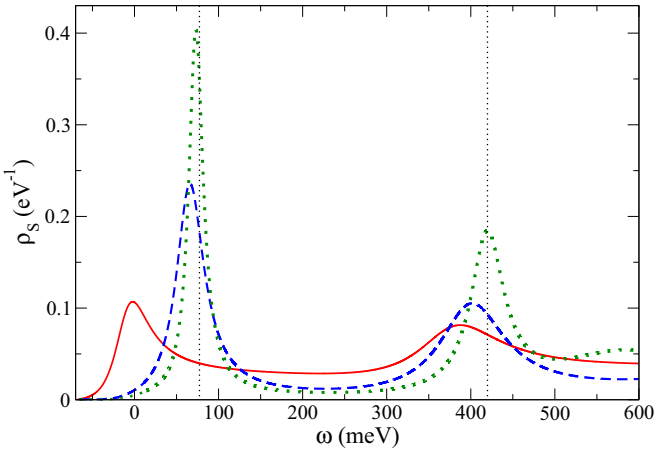

FIG. 11. Full line: theoretical differential conductance as a function of energy for the STM tip in the center of the Ag resonator. Dashed line: the same for a hypothetical closed Ag resonator with five atoms per wall. Dotted line: the same for six atoms per wall. Vertical thin dotted lines correspond to eigenenergies of a hard-wall rectangular corral.

related to discrete states due to confinement in the direction perpendicular to the walls (say x). For hard walls the energies are $E_n = (\pi\hbar n/d_w)^2/(2m^*)$ above the bottom of the surface band ω_B, where $d_w = 5.326$ nm is the distance between the walls. Since only even wave functions can be sensed by the tip on the symmetry axis between the walls, the lowest two levels correspond to $E_1 = -24.2$ meV and $E_3 = 318.4$ meV, similar but smaller to the center of the peaks mentioned above. At high energies the conductance tends to the constant $B\rho_b + S\rho_{s0}$.

Including the one-dimensional motion along the walls (y direction), the surface spectral density per atom becomes

$$\rho_s(\omega) = \frac{\lambda^2\sqrt{2m^*}}{\pi\hbar d_w}\sum_n \frac{\theta(\omega - E_{2n+1})}{\sqrt{\omega - E_{2n+1}}},$$

where $\theta(\omega)$ is the step function. This function is shown in Fig. 10 by a dotted line. By comparison, one can see that for the resonators, the peaks have increasing width as the energy is increased. In fact further peaks (not shown) are quite flat. This fact indicates that the possibility to increase ρ_s is important only near the bottom of the band $\omega_B = -67$ meV. Since in other noble metal surfaces like Cu and Au, $\omega_B \sim -0.5$ eV, the possibility to modify substantially the surface density of states at the Fermi level $\rho_s(0)$ or near it is restricted to the (111) surface of Ag.

In Fig. 10 we also show the change in $\rho_s(\omega)$ when the walls of the resonator are made two times longer, keeping the same density. As longer distances are involved, oscillations of the type already noticed in Fig. 9 appear at lower energy. Apart from this fact, the result indicates that longer walls do not lead to significantly larger surface density, in agreement with experiment.

Another possibility to interpret the resulting density of surface states is to start from the eigenstates of a hard-wall rectangular corral, which become resonances for a leaky corral (in particular if two walls are missing). This has been worked out in detail for a circular soft corral [19]. For a rectangular hard-wall corral of sides a and $b = 3.46$ nm, the eigenstates lie at energies $E_{n,m} = (\pi\hbar)^2/(2m^*)[(n/a)^2 + (m/b)^2] + \omega_B$. The first two states with nonzero amplitude correspond to energies $E_{1,1} = 77.28$ meV, and $E_{1,3} = 419.85$ meV. The first energy lies above the corresponding peak for the resonator. Therefore, it seems that the description of the observed conductance in terms of resonances due to confinement in both directions is not very helpful for open resonators.

In Fig. 11 we show the effect on $\rho_s(\omega)$ if one closes the resonator adding three hypothetical evenly spaced Ag atoms at each open end of the resonator, building a closed rectangle with five atoms at each side. The result is a considerable increase of the intensity of the lowest peak in the spectral density of surface states. However, the peak is also displaced to the value corresponding to a hard wall corral, and as a consequence $\rho_s(0)$ slightly decreases. In any case, this shows the potential of engineering closed resonators. In particular, the main peak can be shifted towards the Fermi energy choosing the dimensions of the rectangular corral in such a way that $E_{1,1} \sim 0$, for example, increasing b from 3.46 nm to 7.1 nm.

We also studied the effect of decreasing hypothetically the distance between Ag atoms, adding more atoms but keeping the same shape of the rectangular resonator. As expected, the peaks become narrower and sharper, particularly at higher energies.

IV. SUMMARY AND DISCUSSION

We have characterized experimentally the changes in the differential conductance observed by a scanning tunneling microscope on the Ag(111) surface when resonators of Co and Ag adatoms are built on the surface. These changes are originated by the effects of the confinement on the electronic structure of the surface Shockley states. The density of these states is enhanced by a factor between 2 and 3 due to confinement.

These effects can be explained by a simple one-particle model, whose main ingredient is an attractive potential W at the positions of the adatoms. This potential is slightly larger

for Ag than for Co. The model contains also a bulk-surface hybridization at the adatom positions W_b that affects the width of the peaks in the surface spectral density. For the positions of the STM tip studied experimentally, the contribution of the surface states to the observed differential conductance is several times larger than that of the bulk states, in spite of the fact that the density of states of the latter is nearly three times larger for a clean surface.

The model allows us to understand the main features of the observed differential conductance in several arrangements of adatoms and to predict the effects on the electronic structure of the surface states expected for new arrangements. In particular, closed resonators in the form of corrals are expected to lead to further enhancement of the spectral density of surface states near the Fermi level. The observed enhancement, and possible further increase of it, is due to the fact that (in contrast to Cu and Au) the surface Shockley states of Ag start slightly below the Fermi level. We also expect that this model can be a starting point to understand the nontrivial effects of confinement on the Kondo effect for magnetic impurities on Ag surfaces.

ACKNOWLEDGMENTS

Two of us (J.F. and A.A.A.) thank CONICET from Argentina for financial support. This work was sponsored by PIP 112-201101-00832 of CONICET and PICT 2013-1045 of the ANPCyT.

[1] D. M. Eigler and E. K. Schweizer, Nature (London) **344**, 524 (1990).
[2] M. F. Crommie, C. P. Lutz, and D. M. Eigler, Science **262**, 218 (1993).
[3] E. J. Heller, M. F. Crommie, C. P. Lutz, and D. M. Eigler, Nature (London) **369**, 464 (1994).
[4] H. C. Manoharan, C. P. Lutz, and D. M. Eigler, Nature (London) **403**, 512 (2000).
[5] G. A. Fiete and E. J. Heller, Rev. Mod. Phys. **75**, 933 (2003); references therein.
[6] A. A. Aligia and A. M. Lobos, J. Phys. Cond. Matt. **17**, S1095 (2005); references therein.
[7] M. Plihal and J. W. Gadzuk, Phys. Rev. B **63**, 085404 (2001).
[8] P. Roushan, J. Seo, C. V. Parker, Y. Hor, D. Hsieh, D. Qian, A. Richardella, M. Z. Hasan, R. Cava, and A. Yazdani, Nature (London) **460**, 1106 (2009).
[9] Y. Takahashi, T. Miyamachi, K. Ienaga, N. Kawamura, A. Ernst, and F. Komori, Phys. Rev. Lett. **116**, 056802 (2016).
[10] S. L. Hulbert, P. D. Johnson, N. G. Stoffel, W. A. Royer, and N. V. Smith, Phys. Rev. B **31**, 6815 (1985).
[11] A. A. Aligia, Phys. Rev. B **64**, 121102(R) (2001).
[12] D. Porras, J. Fernández-Rossier, and C. Tejedor, Phys. Rev. B **63**, 155406 (2001).
[13] M. Weissmann and H. Bonadeo, Physica E (Amsterdam) **10**, 544 (2001).
[14] K. Hallberg, A. A. Correa, and C. A. Balseiro, Phys. Rev. Lett. **88**, 066802 (2002).
[15] A. A. Aligia, Phys. Status Solidi (b) **230**, 415 (2002).
[16] G. Chiappe and A. A. Aligia, Phys. Rev. B **66**, 075421 (2002).
[17] N. Knorr, M. A. Schneider, L. Diekhöner, P. Wahl, and K. Kern, Phys. Rev. Lett. **88**, 096804 (2002).
[18] E. Rossi and D. K. Morr, Phys. Rev. Lett. **97**, 236602 (2006).
[19] A. Lobos and A. A. Aligia, Phys. Rev. B **68**, 035411 (2003).
[20] F. E. Olsson, M. Persson, A. G. Borisov, J.-P. Gauyacq, J. Lagoute, and S. Fölsch, Phys. Rev. Lett. **93**, 206803 (2004).
[21] L. Limot, E. Pehlke, J. Kröger, and R. Berndt, Phys. Rev. Lett. **94**, 036805 (2005).
[22] In the continuum formalism the scattering potential on the surface states takes the form $W\lambda^2 \sum_i \delta(\mathbf{r} - \mathbf{r}_i)$, where $\mathbf{r}_i$ is the two-dimensional vector that describes the position of the adatom i and λ^2 with $\lambda = 2.685$ Å is the area per Ag atom of the (111) surface [6].
[23] A. Schiller and S. Hershfield, Phys. Rev. B **61**, 9036 (2000).
[24] A. A. Aligia, P. Roura-Bas, and S. Florens, Phys. Rev. B **92**, 035404 (2015).
[25] O. Agam and A. Schiller, Phys. Rev. Lett. **86**, 484 (2001).
[26] J. Kliewer, R. Berndt, and S. Crampin, New J. Phys. **3**, 22 (2001).
[27] S. Crampin, H. Jensen, J. Kröger, L. Limot, and R. Berndt, Phys. Rev. B **72**, 035443 (2005).
[28] See, for example, C. Cohen-Tannoudji, B. Diu, and F. Laloë, *Quantum Mechanics*, Vol. 1 (Hermann, Paris, 1977).